FULL PAPER

Dalton
www.rsc.org/dalton

Synthesis, crystal structure and hydroformylation activity of triphenylphosphite modified cobalt catalysts

Marco Haumann,[a] Reinout Meijboom,[a] John R. Moss[b] and Andreas Roodt*[a]

[a] *Department of Chemistry and Biochemistry, Rand Afrikaans University, P.O. Box 524, Auckland Park, South Africa 2006. E-mail: aroo@rau.ac.za; Fax: +27-(0)11-4892819; Tel: +27-(0)11-4893835*

[b] *Department of Chemistry, University of Cape Town, Rondebosch 7701, South Africa*

Received 27th February 2004, Accepted 21st April 2004
First published as an Advance Article on the web 10th May 2004

The dinuclear complex $[Co_2(CO)_6\{P(OPh)_3\}_2]$ (**2**) has been synthesised and was fully characterised. The solid state structure revealed a *trans* diaxial geometry, no bridging carbonyls, and Co–Co and Co–P bond lengths of 2.6722(4) and 2.1224(4) Å, respectively. Catalysed hydroformylation of 1-pentene with **2** was attempted at temperatures in the range 120 to 210 °C and pressures between 34 and 80 bar. High pressure spectroscopy (HP-IR and HP-NMR) was used to detect hydride intermediates. High pressure infrared (HP-IR) studies revealed the formation of $[HCo(CO)_3P(OPh)_3]$ (**4**) at *ca*. 110 °C, but at higher temperatures absorption bands corresponding to $[HCo(CO)_4]$ (**3**) were observed. The hydride intermediate **4** has also been synthesised and characterised. Upon increased ligand concentration, HP-IR studies showed the formation of new carbonyl absorption bands due to a higher substituted cobalt carbonyl complex-$[HCo(CO)_2\{P(OPh)_3\}_2]$ (**5**), which is believed to be catalytically less active. Complex **5** has been synthesised independently and was fully characterised. A low temperature crystal structural study of **5** revealed a trigonal bipyramidal structure with a *trans* H–Co–CO arrangement and two equatorial phosphite ligands, the Co–P bond lengths being 2.1093(8) and 2.1076(8) Å, respectively.

Introduction

The hydroformylation of alkenes, also known as the oxo synthesis, was discovered in 1938 by Otto Roelen at Ruhrchemie.[1] In the hydroformylation reaction, alkenes react with carbon monoxide and hydrogen, in the presence of a transition metal catalyst, to form aldehydes containing an additional carbon atom. Hydroformylation today is the most important application of homogeneous catalysis on an industrial scale,[2] with worldwide production capacities about 6 million ton year^{-1}.

The first generation of catalysts was based on unmodified $[HCo(CO)_4]$, which required high reaction pressures to ensure the stability of the active catalyst and to avoid cobalt plating. In 1966,[3–5] Shell reported a system where the addition of a tertiary phosphine stabilised the catalyst to such an extent that reaction pressures below 100 bar were feasible. These modified systems were less reactive than the unmodified one and resulted in a decrease in reaction rates upon increasing the concentration of ligand. The larger steric demand of the phosphine ligand, compared to CO, led to improved selectivity for the desired linear products.[6] Therefore, the higher selectivities observed at higher ligand/metal ratios could be attributed to an increased concentration of the modified hydride species. However, due to the increased electron density on the cobalt, hydrogenation of the aldehydes led to alcohols as the primary products. This characteristic of the catalyst system can thus also result in hydrogenation of the alkene feedstock, leading to eventual undesired alkane formation.

The origin of selectivity can be explained by the Heck and Breslow mechanism, originally derived for unmodified cobalt catalysis.[7] This mechanism was later generalised and applied to ligand modified systems as well (Scheme 1), in which the catalyst precursor is the mono-substituted hydride, $[HCo(CO)_3L]$ (**4**).

The unsaturated $[HCo(CO)_2L]$ species is formed by loss of a CO ligand, and the addition of an alkene to this 16e species is rapid, resulting in the π-complex (**6**). Hydrogen transfer to the alkene is influenced by the steric demand of the ligand, leading to either Markovnikov or, preferentially, *anti*-Markovnikov addition. In the case of unmodified catalysis, the symmetry of the species should yield equal amounts of linear and branched aldehydes (l/b = 1), and addition of CO produces the alkyl species $[RCH_2CH_2Co(CO)_3L]$ (**7**). Alkyl migration to a coordinated CO ligand results in the acyl species $[R'C(O)Co(CO)_3L]$ (**8**) which is cleaved by hydrogen to form the aldehyde and regenerate the hydride **4**.

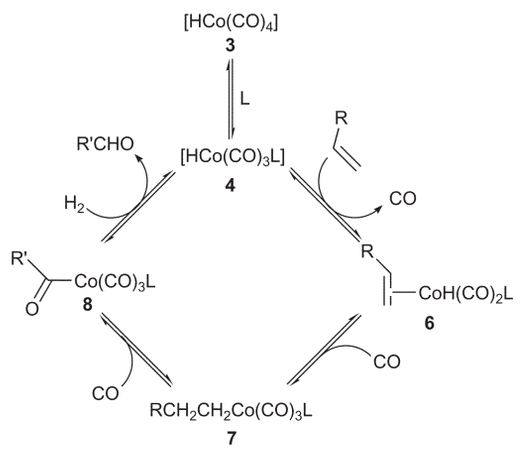

Scheme 1 Generalised Heck–Breslow mechanism.

Since the Shell process which utilised trialkylphosphines was introduced, a variety of phosphine ligands have been studied.[8] Recently the use of tertiary phosphine ligands, in which the phosphorus atom is incorporated in a limonene bicycle, has been reported.[9] Except for one patent from 1967,[10] no reports on the use of phosphite ligands in the cobalt catalysed hydroformylation have appeared. Since phosphites, relative to phosphines, should decrease the electron density on the cobalt centre, they are expected to yield less hydrogenation products. In this paper we report our results on triphenylphosphite modified cobalt hydroformylation studied by HP-NMR, HP-IR, batch autoclave reactions and independent synthesis of the proposed intermediate hydrides $[HCo(CO)_3P(OPh)_3]$ (**4**) and $[HCo(CO)_2\{P(OPh)_3\}_2]$ (**5**).

Experimental

All syntheses of air and moisture sensitive compounds were performed using standard Schlenk techniques under prepurified N_2.[11] Toluene was distilled from Na and tetrahydrofuran from Na/benzophenone/tetraglyme prior to use.[12] All other solvents were used as received. Dicobalt octacarbonyl was purchased from Strem Chemicals and stored under N_2 in a Schlenk-tube wrapped with aluminum foil at 4 °C. The C_9–C_{11} paraffin cut (C_8 3, C_9 26, C_{10} 29, C_{11} 33, C12 9%) and 1-pentene (> 99%), a Fischer–Tropsch

DOI: 10.1039/b403033h

derived product, was supplied by Sasol. Syngas ([CO]/[H_2] = 0.5) was purchased from Afrox. All other reagents were purchased from Sigma–Aldrich and used as received. Melting points were determined on a Kofler hot-stage microscope (Reichert–Thermovar). Elemental analyses were performed using a Carlo Erba EA1108 elemental analyser in the microanalytical laboratory of the University of Cape Town.

X-Ray crystallography data collection and refinement

Crystals of $[Co_2(CO)_6\{P(OPh)_3\}_2]$[13] (**2**) and $[HCo(CO)_2\{P(OPh)_3\}_2]$ (**5**) were grown from THF as described below. X-Ray diffraction data for **2**: collected on a Nonius Kappa CCD diffractometer at 203(2) K with 1.5 kW graphite monochromated MoKα (0.71073 Å) radiation. The strategy for the data collection was evaluated using COLLECT.[14] The data were integrated, scaled and reduced with DENZO-SMN.[15] Data for **5**: collected on a Siemens SMART CCD diffractometer using Mo Kα (0.71073 Å) and ω-scans at 203(2) K. After completed collection, the first 50 frames were repeated to check for decay, which was not observed. All reflections were merged and integrated using SAINT[16] and were corrected for Lorentz, polarization and absorption effects using SADABS.[17] The structures were solved by the heavy atom method and refined through full-matrix least-squares cycles using the SHELXL97[18] software package with $\sum(|F_o|-|F_c|)^2$ being minimised. All non-H atoms were refined with anisotropic displacement parameters, while the H atoms were constrained to parent sites using a riding model, except for the hydrido ligand in **5**, of which the position was determined from a difference Fourier map and refined with an isotropic thermal parameter. The DIAMOND[19] Visual Crystal Structure Information System software was used for the graphics. Crystal data and details of data collection and refinement are given in Table 1.

CCDC reference numbers 232540 and 232541.

See http://www.rsc.org/suppdata/dt/b4/b403033h/ for crystallographic data in CIF or other electronic format.

Synthesis of $[Co_2(CO)_6\{P(OPh)_3\}_2]$ (2)

Compound **2** was synthesised by an adapted literature method.[20] The data are in agreement with the literature,[20] and only new data are reported. A solution of $P(OPh)_3$ (0.998 g; 3.22 mmol) in toluene (5 cm^3) was added to a stirred solution of $Co_2(CO)_8$ (0.502 g; 1.46 mmol) in toluene (10 cm^3). The immediate evolution of gas was observed and a precipitate formed. After 16 h the volatiles were removed *in vacuo* and the remaining solid was washed with pentane (3 × 10 cm^3). The dark red powder was dried *in vacuo* to give pure **2** (1.21 g; 91%). Crystals suitable for X-ray diffraction were obtained from the slow evaporation of a solution of **2** in THF. mp 155 °C (dec.) (Found: C, 55.54; H, 3.06. $C_{42}H_{30}Co_2O_{12}P_2$ requires C, 55.65; H, 3.34%); $\tilde{\nu}_{max}/cm^{-1}$ (CO) 1998 (19), 1979 (100%) (CH_2Cl_2); 1998 (20), 1981 (100%) (1-heptanol); δ_H($CDCl_3$): 7.32, 7.21; $\delta_{C\{H\}}$($CDCl_3$): 200.26 (CO), 151.07, 129.90, 125.78, 121.93; $\delta_{P\{H\}}$($CDCl_3$): 168.2.

Synthesis of $[HCo(CO)_3\{P(OPh)_3\}]$ (4)

(a) *N*,*N*-dimethylformamide (2.0 cm^3; 25.8 mmol) was added to a solution of $[Co_2(CO)_8]$ (0.292 g; 0.851 mmol) in pentane (10 cm^3) and stirred. A pink precipitate formed and the solution decolourised. At 0 °C, 6 M HCl (6.0 cm^3) was added to this mixture and an immediate phase separation was observed. The light yellow organic phase was separated from the dark blue aqueous phase. $P(OPh)_3$ (0.264 g; 0.85 mmol) was added to the organic phase at 0 °C and immediate gas evolution was observed. IR spectroscopy showed that the title compound had formed. The solution was concentrated and stored in the freezer. Crystals of **4** formed and were isolated (0.268 g, 52%). $\tilde{\nu}_{max}/cm^{-1}$ (CO) 2073 (34), 2021 (45), 1997 (100%) (toluene); δ_H($CDCl_3$): 7.30, 7.11 ($P(OPh)_3$), −11.23 (d, H, ^2J(H,P) = 54 Hz); $\delta_{C\{H\}}$($CDCl_3$): 151.62 (*ipso*), 129.51, 124.62 (*para*), 121.86; $\delta_{P\{H\}}$($CDCl_3$): 158.76.

Table 1 Crystal data and structure refinement detail for $[Co_2(CO)_6\{P(OPh)_3\}_2]$ (**2**) and $[HCo(CO)_2\{P(OPh)_3\}_2]$ (**5**)

	2	**5**
Empirical formula	$C_{42}H_{30}Co_2O_{12}P_2$	$C_{38}H_{30}CoO_8P_2$
Formula weight	906.46	1470.98
Temperature (K)	203(2)	203(2)
Wavelength (Å)	0.71073	0.71073
Crystal system, space group	$P\bar{1}$	$P\bar{1}$
a (Å)	9.3422(2)	9.8233(5)
b (Å)	11.0745(2)	10.6474(6)
c (Å)	12.0715(2)	18.5277(11)
α (°)	63.7430(10)	80.813(4)
β (°)	89.6420(10)	81.284(4)
γ (°)	65.7760(10)	64.028(4)
Volume (Å^3)	997.70(3)	1712.52(17)
Z, Calculated density (mg m^{-3})	1, 1.509	2, 1.426
Absorption coefficient (mm^{-1})	0.975	0.648
F(000)	462	758
Crystal size	0.20 × 0.15 × 0.15 mm	0.30 × 0.11 × 0.07 mm
θ range (°)	3.65, 27.46	1.12, 28.35
Index ranges	$-11 \le h \le 12$ $-14 \le k \le 14$ $-15 \le l \le 15$	$-13 \le h \le 13$ $-14 \le k \le 13$ $-24 \le l \le 24$
Reflections collected/unique	8620/4543 [R(int) = 0.0262]	16026/8502 [R(int) = 0.0557]
Completeness to 2θ	99.4%	99.2%
Max. and min. transmission	0.8675 and 0.8288	—
Refinement method	Full-matrix least-squares on F^2	Full-matrix least-squares on F^2
Data/restraints/parameters	4543/0/262	8502/0/446
Goodness-of-fit on F^2	1.004	0.908
Final R indices [$I > 2\sigma$(I)]	$R1$ = 0.0293, $wR2$ = 0.058	$R1$ = 0.0489, $wR2$ = 0.0825
R indices (all data)	$R1$ = 0.0501, $wR2$ = 0.0640	$R1$ = 0.1147, $wR2$ = 0.0983
Largest diff. peak and hole/e Å^{-3}	0.271 and −0.285	0.507 and −0.535

(b) The compound was prepared according to a modification of the literature methods,[21] reacting the $Na[Co(CO)_3P(OPh)_3]$, generated from **2**, with 1.0 M HCl in Et_2O. The attempted reduction of the dimer (**2**) using stronger reducing agents (Na/K melt; K- or Na-sand) was not successful. All analytical data were in accordance with literature[21] and the product obtained using method (a).

Synthesis of $[HCo(CO)_2\{P(OPh)_3\}_2]$ (5)

(a) The synthesis for compound **4** was repeated with 2 equivalents of $P(OPh)_3$. Compound **5** precipitated immediately from pentane upon addition of $P(OPh)_3$. Removal of the pentane followed by additional washing with small amounts of pentane afforded pure **5** (95%). Crystals suitable for X-ray diffraction were obtained by slow diffusion of pentane into a solution of **5** in toluene. $\tilde{\nu}_{max}/cm^{-1}$ (CO) 2034 (100), 1996 (78), 1971 (98%) (toluene); δ_H($CDCl_3$): 7.30; 7.11 ($P(OPh)_3$), −11.98 (1H, t, ^2J(H,P) = 12 Hz); δ_H(C_6D_6): −11.9 (1H, t, ^2J(H,P) = 12 Hz); $\delta_{C\{H\}}$($CDCl_3$): 151.62 (*ipso*), 129.51, 124.62 (*para*), 121.86; $\delta_{P\{H\}}$($CDCl_3$): 157.8.

(b) The compound was prepared according to a modification of the literature methods,[22] reacting the $Na[Co(CO)_3P(OPh)_3]$ generated from **2** with $POCl_3$ and $P(OPh)_3$ at −78 °C to give $Cl[Co(CO)_2\{P(OPh)_3\}_2]$. The compound $Cl[Co(CO)_2\{P(OPh)_3\}_2]$ was then reacted with Na/Hg, followed by reaction with HCl in Et_2O to give the title compound. All analytical data were in agreement with that found for method (a).

Infrared experiments

All infrared spectra were recorded on a Bruker Equinox 55 FT-IR spectrometer and analysed with the Bruker OPUS-NT software (32 scans, 4 cm^{-1} resolution, Blackman-Harris 3-Term apodization). Infrared data for solution spectra of compounds **2** to **5** were collected using NaCl windows (optical pathlength 0.1 mm). The high-pressure experiments were carried out in a 55 cm^3 SS 316 autoclave equipped with a mechanical stirrer (750 rpm), a temperature, and

a pressure control (University of Amsterdam).[23] The solution was pumped through a bypass, in which ZnS windows were embedded (optical pathlength at 25 °C: 0.3 mm).

The autoclave was flushed with argon prior to use. A solution of dimer **2** ([Co] = 1500 ppm, mg/kg solvent, in the final volume) in 10 cm^3 degassed solvent was transferred under argon into the autoclave. The appropriate amount of ligand was added and the assembled autoclave was purged with syngas three times. The autoclave was then pressurised at room temperature to 15 bar, resulting in a final pressure of approximately 20 bar at 140 °C. When the autoclave had reached reaction temperature, 2 cm^3 pentene was injected from an attached sample reservoir to give a total reaction pressure of 50 bar syngas. After the reaction, GC samples were taken from the cooled and depressurised solution. ^{31}P NMR spectra of samples taken from the cooled and depressurised solution showed the presence of only compounds **2** and **5** and free $P(OPh)_3$.

NMR experiments

NMR spectra were recorded on a Varian Inova 300 MHz spectrometer (^1H: 300 MHz, ^{13}C: 75.5 MHz, ^{31}P: 121.5 MHz) spectrometer at ambient temperature. NMR spectra were referenced relative to TMS (^1H and ^{13}C) or 85 % H_3PO_4 (^{31}P) using either the residual protonated impurities in the solvent (^1H NMR: $CDCl_3$: δ 7.27; C_6D_6: δ 7.16), the solvent resonances (^{13}C NMR: $CDCl_3$: δ 77.0; C_6D_6: δ 128.0) or external (^{31}P). The high pressure NMR experiments were performed in a 10 mm high pressure Roe cell.[24] For these high pressure experiments, the required amount of dimer (**2**) was weighed in an argon-filled sample tube, dissolved in 1 cm^3 C_6D_6 and transferred into the NMR tube via syringe. The appropriate amount of $P(OPh)_3$ was dissolved in 1 cm^3 C_6D_6 and transferred under argon into the NMR tube. The cell was purged three times with syngas, pressurised to 40 bar and left under pressure overnight (approximately 15 hours) to allow proper gas dissolution.

Batch autoclave experiments

The stainless steel 300 cm^3 autoclave (Parr model 4560) was flushed with argon prior to use. The electrically heated autoclave was equipped with a magnetic drive stirrer, sampling dip tube and internal cooling coil. The required amounts of the dimer (**2**) and $P(OPh)_3$ were dissolved in 75 cm^3 degassed solvent. The closed autoclave was then purged three times with syngas and pressurised to 20 bar, resulting in 30 bar pressure at 140 °C. 1-Pentene (100 cm^3, 0.91 mol) was injected from a 150 cm^3 sample cylinder kept under 50 bar syngas pressure. The reaction pressure of 50 bar was maintained by constant addition of consumed gas. Samples were taken at intervals into a sampling tube, which was cooled (4 °C) to prevent evaporation of 1-pentene. The samples were analysed by gas chromatography using an Agilent 6890 series GC system equipped with a Hewlett Packard Pona column (50 m × 0.5 μm) and FID detection method. Temperature program: 100 °C (10 min hold), 250 °C (2 °C min^{-1}), 250 °C (5 min hold), 300 °C (10 °C min^{-1}), 300 °C (5 min). The N_2 carrier gas flow was kept constant at 0.7 cm^3 min^{-1}.

Results and discussion

Synthesis

The dinuclear complex $[Co_2(CO)_6\{P(OPh)_3\}_2]$ (**2**) was synthesised from dicobalt octacarbonyl and an excess triphenylphosphite,[20] and fully characterised by IR, NMR, elemental analysis and X-ray crystallography. The molecular diagram of **2** is shown in Fig. 1. Compound **2** was used as starting material for the HP-IR, HP-NMR and batch autoclave reactions.

The hydride complexes $[HCo(CO)_3P(OPh)_3]$ (**4**) and $[HCo(CO)_2[P(OPh)_3]_2]$ (**5**) were prepared using two different synthetic routes (see Scheme 2). The main reason for using route (b) for the synthesis of **4** and **5** was to illustrate that reduction of **2** (by H_2 under catalytic conditions) can lead to the formation of both **4** and **5**. Both **4** and **5** were isolated as crystalline pale yellow

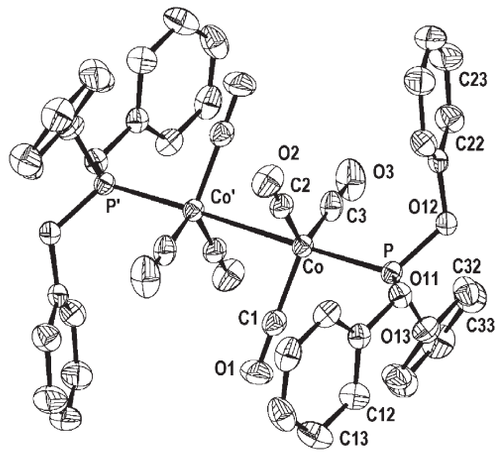

Fig. 1 Molecular diagram of $[Co_2(CO)_6\{P(OPh)_3\}_2]$ (**2**).

solids and crystals suitable for X-ray diffraction of **5** (see Fig. 2) were grown from slow diffusion of pentane into a solution of **5** in toluene. Compound **4** was thermally sensitive at atmospheric pressure and dimerised above 0 °C as a solid and at −20 °C in solution to form **2**. This thermal sensitivity prevented us from obtaining crystals of **4** suitable for X-ray crystallography. Compound **5** was thermally more stable (decomposed slowly as a solid at 20 °C) but also decomposed rapidly in solution (20 °C). Complexes **4** and **5** are both moderately oxygen sensitive, but not sensitive toward water, and could be identified by HP-IR and HP-NMR with ease. The chemical shift for the hydrido ligand and the coupling to P (**4**: δ −11.2, d; **5**: δ −11.9, t; $[HCo(CO)_4]$ (**3**): δ −11.4, s) could be used to easily distinguish between the different hydrides (see also Fig. 5 later). The ν_{CO} absorptions of the various hydrides were also sufficiently different to enable separate detection by HP-IR.

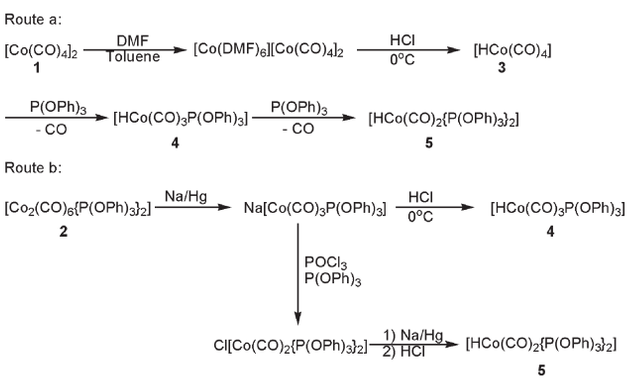

Scheme 2 Synthesis of **4** and **5**.

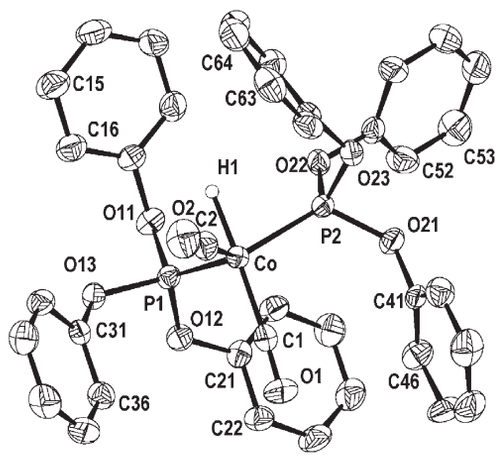

Fig. 2 Molecular diagram of $[HCo(CO)_2\{P(OPh)_3\}_2]$ (**5**).

Solid state structures of 2 and 5

Molecular diagrams showing the numbering schemes and thermal ellipsoids for **2** and **5** are given in Fig. 1 and 2, respectively. Selected geometrical parameters are summarised in Table 2 and 3.

The molecular diagram of **2** (Fig. 1) clearly shows its dinuclear arrangement, formed by two trigonal [−$Co(CO)_3${$P(OPh)_3$}] fragments, with the two $P(OPh)_3$ ligands occupying *trans* configurations with respect to the Co–Co bond (2.6722(4) Å). The molecule lies on a centre of symmetry which bisects the Co–Co bond, and the $P(OPh)_3$ ligands have a measured cone angle of 175°. A trigonal plane is defined by the three carbonyl ligands and the Co atom is displaced by 0.158(1) Å towards the apical $P(OPh)_3$.

Complex **5** represents a rare and first example of a hydride structure of cobalt(I) stabilised by $P(OPh)_3$ ligands. The complex exhibits a severely distorted trigonal bipyramidal structure with the two $P(OPh)_3$ ligands and one carbonyl occupying the plane. The hydride and the other carbonyl are in a *trans* orientation (H1–Co–C1 = 177.9(13)°) in the apical positions relative to the trigonal plane. The cobalt atom is displaced by 0.320(1) Å from the trigonal plane away from the hydride ligand.

The Co–P bond in **2** (*trans* to the Co–Co bond) of 2.1224(4) Å is significantly longer that the Co–P(1) and Co–P(2) bonds (2.1093(8) and 2.1076(8) Å respectively) in **5**, indicative of the *trans* influence exerted by the Co–Co metal bond. This is further illustrated by the shortening of the P–O bonds in **2** (1.5977(12), 1.6012(12), and 1.6029(11) Å) compared to those in **5** ranging from 1.609(2) to 1.635(2) Å.

The Co–C(1) bond trans to the Co–H moiety in **5** is shortened (1.758(3) Å) compared to the Co–C(2) bond (1.775(3) Å) in the hydride complex, indicating increased π back bonding in the *trans* H–Co–CO fragment. The Co–C(2) bond is comparable with the three Co–CO bonds in **2**, which range from 1.780(2) to 1.787(2) Å.

Table 4 illustrates the geometric parameters of **2** and **5** as compared with other examples from literature. The distortion induced in these types of complexes is clear: more bulky ligands showing more significant effects.

The distortion due to the (sterically demanding) phosphorus donor ligands (large cone angles) is manifested in the displacement of the Co atom from the trigonal plane formed by the three CO ligands in the dimeric complexes, as well as the P–Co–CO angle (Table 4(a)). This is particularly observed in complex **2** and $[Co_2(CO)_6(PMe_3)_2]$.[28] Similar distortion is observed for the hydride species (Table 4(b)), where the Co atom is displaced from the trigonal plane, possibly as a result of the large cone angle of the phosphorus donor ligands. We are currently further investigating the influence of phosphorus donor ligands on the out-of-plane displacement of cobalt atoms in associated complexes.

HP-IR experiments

The formation of $[HCo(CO)_3P(OPh)_3]$ (**4**) was studied at various ligand/metal ratios by adding the appropriate amount of $P(OPh)_3$ to the dinuclear complex $[Co_2(CO)_6${$P(OPh)_3$}$_2]$ (**2**). The monosubstituted hydride **4**, indicated by absorbances at 2071, 2021 and 2001 cm^{-1}, was formed at similar temperatures of 120 °C in both toluene and paraffin (Fig. 3a). Table 5 summarises the results obtained in the solvents toluene, C_9–C_{11} paraffins and 1-heptanol. The concentration was kept constant throughout the experiments at 1500 ppm Co with the $[P(OPh)_3]$/[Co] ratio varying between 1 and 20 (50 for paraffin). The formation of the hydride species was studied up to 140 °C and 50 bar of syngas pressure.

The ν_{CO} absorption at 1983 cm^{-1} was used as an indicator for the dimeric $[Co_2(CO)_6${$P(OPh)_3$}$_2]$ (**2**). In both toluene and paraffin at 120 °C, this peak decreased in a synchronised way when hydride **4** was formed and disappeared completely around 140 °C, independent of ligand excess. The lowest $[P(OPh)_3]$/[Co] ratio to prevent the formation of $[HCo(CO)_4]$ (**3**) was 4, as can be seen from entries 2 to 7 and 10 to 14 in Table 5, where no absorptions for the unmodified hydride could be detected at 2053 and 2030 cm^{-1}.

Table 2 Selected bond lengths (Å) and angles (°) for $[Co_2(CO)_6${$P(OPh)_3$}$_2]$ (**2**)

Co–C(1)	1.785(2)	P–O(13)	1.6029(11)
Co–C(2)	1.7874(19)	C(1)–O(1)	1.148(2)
Co–C(3)	1.780(2)	C(2)–O(2)	1.143(2)
Co–P	2.1224(4)	C(3)–O(3)	1.147(2)
Co–Co^a	2.6722(4)	O(11)–C(11)	1.409(2)
P–O(11)	1.6012(12)	O(12)–C(21)	1.411(2)
P–O(12)	1.5977(12)	O(13)–C(31)	1.413(2)
C(1)–Co–C(2)	117.47(8)	O(2)–C(2)–Co	178.57(17)
C(3)–Co–C(1)	119.61(9)	O(3)–C(3)–Co	179.11(17)
C(3)–Co–C(2)	120.61(9)	O(12)–P–Co	118.79(5)
C(3)–Co–P	93.88(6)	O(11)–P–Co	119.18(5)
C(1)–Co–P	95.48(6)	O(13)–P–Co	118.00(5)
C(2)–Co–P	95.87(6)	C(11)–O(11)–P	123.16(10)
C(3)–Co–Co^a	83.44(6)	C(21)–O(12)–P	123.29(10)
C(1)–Co–Co^a	85.98(6)	C(31)–O(13)–P	121.59(10)
C(2)–Co–Co^a	85.42(5)	O(11)–P–O(13)	99.00(6)
P–Co–Co^a	177.319(19)	O(12)–P–O(11)	98.57(6)
O(1)–C(1)–Co	179.43(17)	O(12)–P–O(13)	99.18(6)

Symmetry code: $^a = 2 - x, 1 - y, 1 - z$.

Table 3 Selected bond lengths (Å) and angles (°) for $[HCo(CO)_2${$P(OPh)_3$}$_2]$ (**5**)

Co–C(1)	1.758(3)	P(2)–O(23)	1.635(2)
Co–C(2)	1.775(3)	C(1)–O(1)	1.157(3)
Co–P(1)	2.1093(8)	C(2)–O(2)	1.147(3)
Co–P(2)	2.1076(8)	O(11)–C(11)	1.410(3)
Co–H(1)	1.45(3)	O(12)–C(21)	1.402(3)
P(1)–O(12)	1.6124(19)	O(13)–C(31)	1.403(3)
P(1)–O(11)	1.6210(18)	O(21)–C(41)	1.404(3)
P(1)–O(13)	1.6215(18)	O(22)–C(51)	1.408(3)
P(2)–O(21)	1.6094(18)	O(23)–C(61)	1.408(3)
P(2)–O(22)	1.6156(18)		
C(1)–Co–C(2)	95.25(13)	O(21)–P(2)–Co	123.72(8)
C(1)–Co–P(2)	103.66(9)	O(22)–P(2)–Co	116.90(8)
C(2)–Co–P(2)	118.87(10)	O(23)–P(2)–Co	116.65(7)
C(1)–Co–P(1)	98.91(10)	C(11)–O(11)–P(1)	120.85(16)
C(2)–Co–P(1)	116.94(10)	C(21)–O(12)–P(1)	125.67(18)
P(2)–Co–P(1)	116.54(3)	C(31)–O(13)–P(1)	121.55(15)
C(1)–Co–H(1)	177.9(13)	C(41)–O(21)–P(2)	124.38(15)
C(2)–Co–H(1)	82.9(13)	C(51)–O(22)–P(2)	124.05(16)
P(2)–Co–H(1)	78.2(13)	C(61)–O(23)–P(2)	121.22(17)
P(1)–Co–H(1)	81.1(14)	O(11)–P(1)–O(13)	97.07(9)
O(1)–C(1)–Co	175.6(2)	O(12)–P(1)–O(11)	97.86(10)
O(2)–C(2)–Co	178.7(3)	O(12)–P(1)–O(13)	96.22(10)
O(11)–P(1)–Co	120.46(8)	O(21)–P(2)–O(22)	96.58(9)
O(12)–P(1)–Co	120.93(8)	O(21)–P(2)–O(23)	96.89(11)
O(13)–P(1)–Co	118.86(7)	O(22)–P(2)–O(23)	101.76(10)

The disubstituted hydride species $[HCo(CO)_2${$P(OPh)_3$}$_2]$ (**5**) was formed in the presence of ligand excess larger than 2 in paraffin (Fig. 3b), which was attributed to the small Tolman cone angle[32] of $P(OPh)_3$ of 124°. In toluene, the characteristic ν_{CO} absorption bands at 2034, 2000 and 1973 cm^{-1} for **5** could be detected even at a ligand/metal ratio of 1 as shown by entry 1 in Table 5.

The formation of $[HCo(CO)_3P(OPh)_3]$ (**4**) and $[HCo(CO)_2${$P(OPh)_3$}$_2]$ (**5**) occurred at the same temperature (120 °C) in toluene, while in paraffin, the required temperature for the formation of the disubstituted hydride **5** decreased slightly with increasing ligand excess from 130 °C to 105 °C.

The hydroformylation activity of the system was studied for various $[P(OPh)_3]$/[Co] ratios both in toluene ($[P(OPh)_3]$/[Co] = 4, 8, 20) and paraffin ($[P(OPh)_3]$/[Co] = 2, 4, 8, 20, 50). 1-Pentene (2 cm^3, 15 mmol) was injected into a solution which has been kept at 140 °C and 20 bar for 30 min to ensure complete conversion of the dimeric substrate **2**. For $[P(OPh)_3]$/[Co] ratios below 20 an immediate formation of aldehyde was detected, indicated by a strong absorbance at 1734 cm^{-1} (Fig. 4), upon addition of 1-pentene.

Following the decrease of the alkene absorption at 1640 cm^{-1} over time revealed a linear rate dependence with ligand excess. With the exception of entry 8 (Table 5) there was no unmodified hydride **3** present under the conditions applied in all (HP-IR) hydroformylation experiments. A $[P(OPh)_3]$/[Co] ratio of 4 was sufficient

Table 4 Structural correlation for (a) $[Co_2(CO)_6\{L\}_2]$ (L = PX_3; CO X = alkyl, aryl, alkoxyl or aroyl) and (b) $[HCo(CO)_2\{L\}_2]$ type complexes

(a) $[Co_2(CO)_6\{\mathbf{L}\}_2]$

	Distances/Å				Angles/°	
L	Co–Co	Co–P	Co–(CO)[a]	dis[b]	P–Co–CO	P–Co–Co*
CO[25]	2.522(1)	—	1.82(1); 1.93(1)[c]	—[d]	—	—
$P(OPh)_3$	2.6722(4)	2.1224(4)	1.783(2)	0.158(1)	95.0	177.3(2)
$P(O^iPr)_3$[26]	2.6544(12)	2.1350(12)	1.769(2)	0.070	92.3	177.00(6)
$P(^nBu)_3$[27]	2.665(14)	2.178(15)	1.75(3)	—	—	180
PMe_3[28]	2.669(1)	2.175(1)	1.772(3)	0.104	93.4	180

[a] Average of equivalent values. [b] Distance of Co from trigonal plane as calculated from data obtained from CSD. [c] Bridging CO. [d] Square pyramidal geometry due to bridging CO ligands.

(b) $[HCo(CO)_2\{\mathbf{L}\}_2]$

	Distances/Å				Angles/°	
L	(C–O) *trans* H	C–O tbp plane	Co–H	Co–P	dis[e]	P–Co–P
$P(OPh)_3$	1.758(3)	1.775(3)	1.45(3)	2.1093(8) 2.1076(8)	0.320(1)	116.54(3)
$P(Ph)_3$[29]	1.767(3)	1.751(3)	1.37(3)	2.185(1) 2.200(1)	0.289	122.6(1)
$P(Ph)_3$[f]	1.781(2)[g]	1.755(3)	1.45(3)	2.153(1) 2.145(1)	—[f]	139.8(1)
$P(o\text{–}Ph\text{–}OC_6H_4)_3$[h]	—	1.779(6)	1.497(5)	2.216(3)	—	—
$P(Cy)_3$[i]	—	1.759(3) 1.767(3) 1.779(3)	1.43(3)	2.2347(7)	0.262	—

[e] Distance of Co from trigonal plane as calculated from data obtained from CSD. [f] A square pyramidal solid state form for $[HCo(CO)_2(PPh_3)_2]$ was also isolated.[29] [g] Apical distance. [h] Mono phosphite hydrido species: $[HCo(CO)_3\{P(o\text{–}Ph\text{–}OC_6H_4)_3\}]$, *trans* H–Co–$PX_3$ moiety; no structure available in CSD.[30] [i] Mono phosphine hydrido species: $[HCo(CO)_3(PCy_3)]$, *trans* H–Co–PX_3 moiety.[31]

Table 5 Results of HP-IR studies on the formation of **4, 5** and **3** under 50 bar syngas

Entry	Solvent	L : M	T_{MH} / °C[a]	T_{DH} / °C[b]	T_{Dimer} / °C[c]	T_{UH} / °C[d]	Pentene
1	Toluene	1	120	105	135	130	No
2		4	125	125	145	n.d.[e]	Yes
3[f]		4	125	120	145	n.d.	Yes
4		8	120	115	140	n.d.	Yes
5		15	125	120	135	n.d.	No
6		17	130	125	140	n.d.	No
7		20	125	125	135	n.d.	Yes
8	Paraffin	1	123	n.d.	140	135	No
9		2	122	n.d.	140	135	Yes
10		4	125	125	140	n.d.	Yes
11		8	122	120	140	n.d.	Yes
12		20	120	120	140	n.d.	No[g]
13		20	130	120	140	n.d.	Yes
14		50	n.d.	105	130	n.d.	Yes
15	1-Heptanol	4	n.d.	n.d.	120	n.d.	Yes
16		8	n.d.	n.d.	120	n.d.	Yes
17		20	n.d.	n.d.	115	n.d.	No

[a] Temperature where $[HCo(CO)_3P(OPh)_3]$ (**4**) appeared. [b] Temperature where $[HCo(CO)_2\{P(OPh)_3\}_2]$ (**5**) appeared. [c] Temperature where absorption of dimer **2** at ν_{CO} 1983 cm^{-1} disappeared completely. [d] Temperature where $[HCo(CO)_4]$ (**3**) appeared. [e] Not detected. [f] 1600 ppm cobalt. [g] 2 cm^3 1-heptanol added.

to prevent the formation of unmodified hydride **3**. However, the disubstituted hydride **5** formed under these conditions as well, but was converted into the monosubstituted hydride **4** as indicated by the decrease in absorbance at 2034 cm^{-1}. This absorption band became less pronounced (sh) while the bands at 2071, 2021 and 2000 cm^{-1} became more dominant, as depicted in Fig. 4.

Under industrial hydroformylation conditions using ligand modified cobalt catalysts, the formed aldehydes are converted into the corresponding alcohols.[33] In order to study the influence of an increased alcohol concentration, 1-heptanol was used as solvent. C_6 alcohols (1-hexanol and 2-methyl-1-pentanol) formed by 1-pentene hydroformylation and consecutive hydrogenation could be separated from this solvent in GC measurements. Since a minimum $[P(OPh)_3]/[Co]$ ratio of 4 was required to prevent formation of $[HCo(CO)_4]$ (**3**), experiments were carried out with $[P(OPh)_3]/[Co]$ = 4, 8 and 20 (entries 15 to 17, Table 5). In the pure 1-heptanol no hydride species could be detected, neither the mono- (**4**) nor the disubstituted (**5**) hydrides. However, at temperatures above 110 °C a new species was being formed, exhibiting a strong ν_{CO} absorption at 1969 cm^{-1}. The same product was formed upon heating **5** in 1-heptanol.[34] The reaction product of **5** with 1-heptanol appeared to be inactive in the hydroformylation of 1-pentene (entry 17, Table 5).

The effect of lower concentrations of alcohol (low conversions) on the catalyst system was investigated by adding 2 cm^3 of 1-heptanol to a paraffin solution containing a 20 fold ligand excess at 120 °C and 50 bar (entry 12). Under these conditions $[HCo(CO)_3P(OPh)_3]$ (**4**) and $[HCo(CO)_2\{P(OPh)_3\}_2]$ (**5**) were present in equilibrium. Alcohol addition led to the formation of the species exhibiting the absorption at 1969 cm^{-1}.

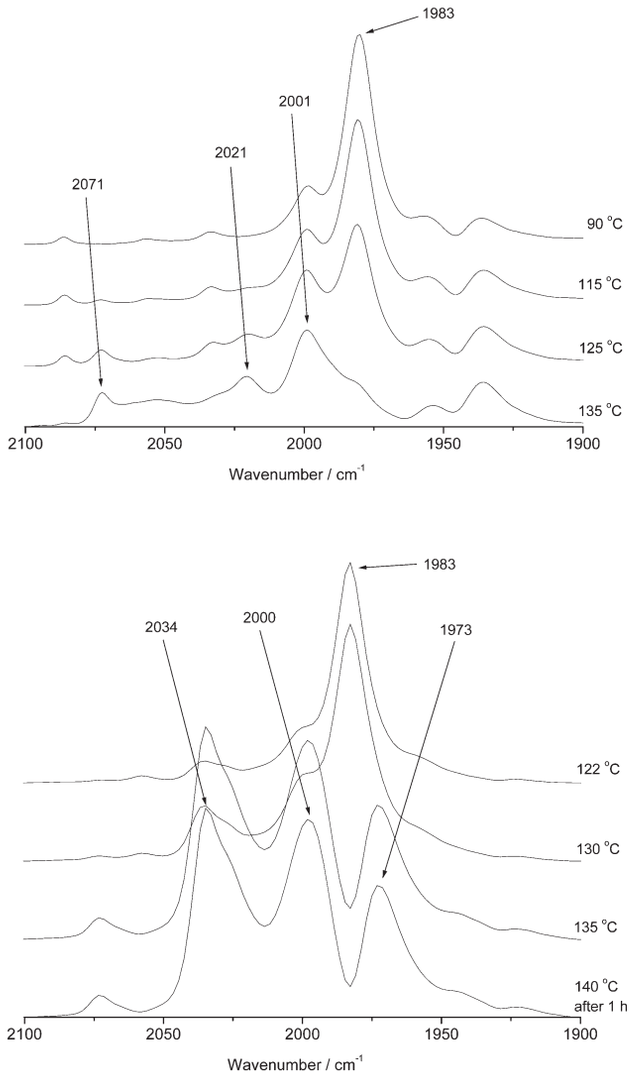

Fig. 3 HP-IR spectra illustrating the formation of **4** and **5**: Top: formation of **4** in toluene at $[P(OPh)_3]/[Co] = 1$ and bottom: formation of **5** in paraffin at $[P(OPh)_3]/[Co] = 8$; [Co] = 1500 ppm in both top and bottom.

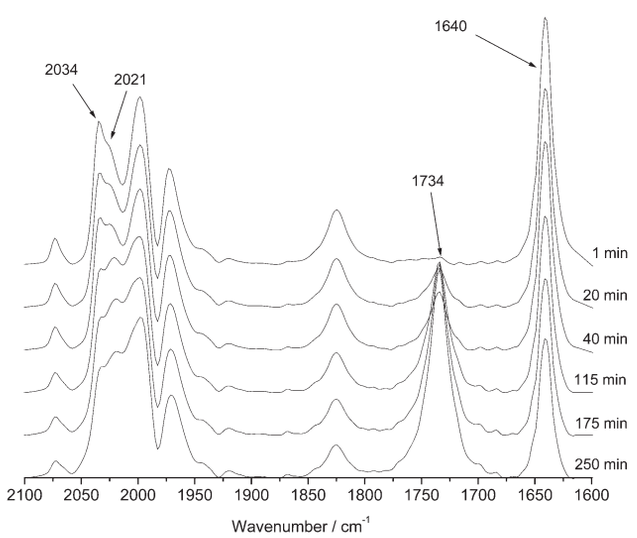

Fig. 4 Hydroformylation of 1-pentene at 140 °C and 40 bar syngas; [Co] = 1500 ppm, $[P(OPh)_3]/[Co] = 8$, [1-pentene]/[Co] = 70.

HP-NMR experiments

All *in situ* experiments were carried out in the high pressure sapphire tube by observing the ^{31}P and ^{1}H nuclei. The concentration of cobalt was kept constant at 1500 ppm and $[P(OPh)_3]/[Co]$ ratios of 1, 4 and 8. Spectra were recorded between 100 and 140 °C with a 30 min hold at each temperature. Peak assignment for the different hydride species was in good agreement with literature results ($[HCo(CO)_4]$ (**3**)) and independent synthesis of $[HCo(CO)_3P(OPh)_3]$ (**4**) and $[HCo(CO)_2\{P(OPh)_3\}_2]$ (**5**). At $[P(OPh)_3]/[Co] = 1$ the ^{31}P spectra showed the presence of dimer **2** at δ 168 ppm, disubstituted hydride **5** at δ 158 ppm and free ligand at δ 126 ppm within the temperature range of 100 to 140 °C. The ^{1}H spectra confirmed these observations showing only two signals at δ −11.9 ppm (**5**) and δ −11.4 ppm (**3**), respectively (Fig. 5). The monosubstituted hydride was not observed, indicating a possible rapid equilibrium under these conditions towards compounds **3** and **5**.

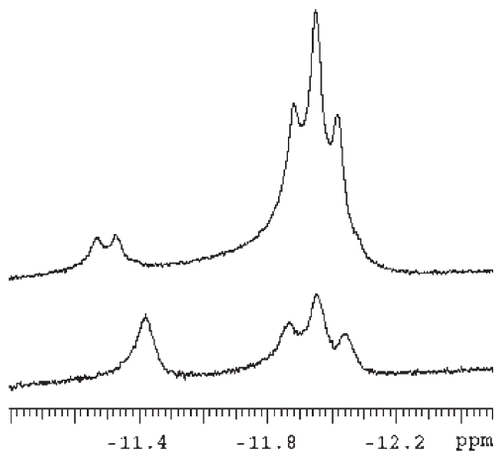

Fig. 5 HP ^{1}H NMR spectra at 130 ºC (50 bar, bottom) and 25 ºC (40 bar, top) at [Co] = 1500 ppm, $[P(OPh)_3]/[Co] = 4$ in C_6D_6.

The presence of dimer **2** at 140 °C and 50 bar agreed with HP-IR studies (see Fig. 3). However, the formation of unmodified hydride **3** was observed only at temperatures above 135 °C in the HP-IR. Moreover, the monosubstituted hydride **4** was clearly present in the infrared studies as depicted in Fig. 3. The discrepancy between the HP-IR and the HP-NMR results stems most probably from differences in heat dissipation and agitation, and thus gas dissolution.

Similar results were observed in the HP-IR for $[P(OPh)_3]/[Co]$ ratios of 4 and 8 (see entries 10 and 11, Table 5), and was reflected in the HP-NMR studies as well. In the ^{1}H spectra the dominant species under the conditions applied was the disubstituted hydride **5**, indicated by a triplet at δ −11.9 ppm (Fig. 5). The unsubstituted hydride **3** was detected as well at δ −11.4 ppm at temperatures between 100 and 140 °C. Due to the strong absorbance at 2034 cm^{-1} of **5**, the band at 2030 cm^{-1} of very small amounts of $[HCo(CO)_4]$ might be obscured. In the ^{31}P spectra the only peaks present were the ones for dimer **2** (δ 168 ppm) and free ligand (δ 126 ppm). Due to the poor signal to noise ratio, the broad peak around δ 158 ppm could not be unambiguously attributed to the disubstituted hydride **5**.

The ^{1}H spectra of both $[P(OPh)_3]/[Co]$ ratios of 4 and 8 taken after cooling to room temperature revealed that the dominant species were the mono- and disubstituted hydride only as indicated by a doublet at δ −11.2 ppm (**4**) and a triplet at δ −11.9 ppm (**5**). Fig. 5 shows the combined ^{1}H spectra of both experiments at 130 °C and 25 °C for [Co] = 1500 ppm and a $[P(OPh)_3]/[Co]$ ratio of 4.

Batch autoclave experiments

Batch autoclave experiments were carried out using paraffin and 1-heptanol as solvent. Samples were taken over a period of 4 h reaction time. Gas chromatography analysis resulted in conversion–time curves as depicted in Fig. 6 for a $[P(OPh)_3]/[Co]$ ratio of 4 in paraffin.

From these curves, the observed rate constant for the pentene conversion was obtained according to the first order rate law

$$-\frac{\mathrm{d[pentene]}}{\mathrm{d}t} = k_{\mathrm{obs}}[\mathrm{pentene}]$$

The results of the batch autoclave hydroformylation experiments are given in Table 6. All internal alkenes were summarised and are given as internals or % isomerisation, respectively. Only selectivities and linearities at the end of the run (EOR) are given.

Table 6 Hydroformylation results for batch autoclave experiments at 140 °C

Entry	c_{Cobalt} ppm	L:M	Hexanals %[a]	Hexanals l/b[b]	Hexanols %[a]	Hexanols l/b[b]	Linearity %[c]	Internals %[a]	TOF h^{-1}[d]	k_{obs} $10^3\ s^{-1}$[e]
18	500	4	3.3	3.3	n.d.[f]	n.d.	77.0	22.8	1.2	0.25
19	500	8	2.5	3.8	n.d.	n.d.	83.4	14.8	1.2	0.10
20	1000	0	49.1	1.0	2.7	1.2	51.3	45.6	32.7	3.22
21	1000	1	16.1	1.9	1.2	2.4	66.6	50.8	4.9	0.63
22	1000	2	26.7	3.6	10.4	3.3	80.8	26.6	2.7	0.38
23	1000	4	5.4	3.7	n.d.	n.d.	70.3	34.2	0.8	0.27
24	1000	8	3.4	4.1	n.d.	n.d.	78.5	27.1	0.6	0.13
25	1000	20	3.6	4.6	n.d.	n.d.	64.7	16.2	0.6	0.05
26	1600	2	5.8	3.1	n.d.	n.d.	75.2	31.8	0.4	0.24
27	1600	4	13.5	4.2	n.d.	n.d.	80.7	18.2	1.7	0.19
28	1600	8	7.1	4.1	n.d.	n.d.	79.7	28.5	0.9	0.17
29[g]	1000	4	n.d.	n.d.	n.d.	n.d.	n.d.	n.d.	n.d.	n.d.
30[h]	1000	8	n.d.	n.d.	n.d.	n.d.	n.d.	n.d.	n.d.	n.d.

[a] Mol%. [b] Linear/branched ratio. [c] Linearity L = linear product/total products. [d] Turn-over frequency TOF = mol (aldehyde + alcohol)/mol cobalt × time. [e] From data fitting. [f] Not detected. [g] 1-Heptanol as solvent at 140 °C. [h] 1-Heptanol as solvent at 170 °C.

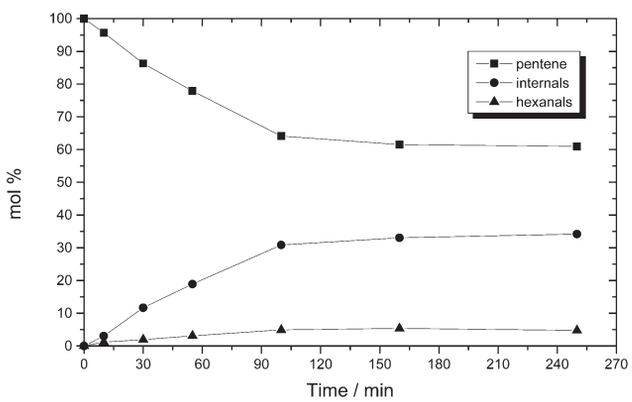

Fig. 6 Hydroformylation of 1-pentene in paraffin followed by GC. 140 °C, 50 bar, [Co] = 1000 ppm, $[P(OPh)_3]/[Co] = 4$.

At a cobalt concentration of 1000 ppm (12.2 mM) the $[P(OPh)_3]/[Co]$ ratio was varied between 2 and 20 (entries 20 to 23). In general the TOF for the cobalt system is very low compared with industrial values (*ca.* 1000 h^{-1}). Aldehydes are produced only to a small extent; the main products under the conditions applied are internal alkenes, derived by isomerisation. The generalised Heck–Breslow mechanism was used to explain these results (Scheme 3).

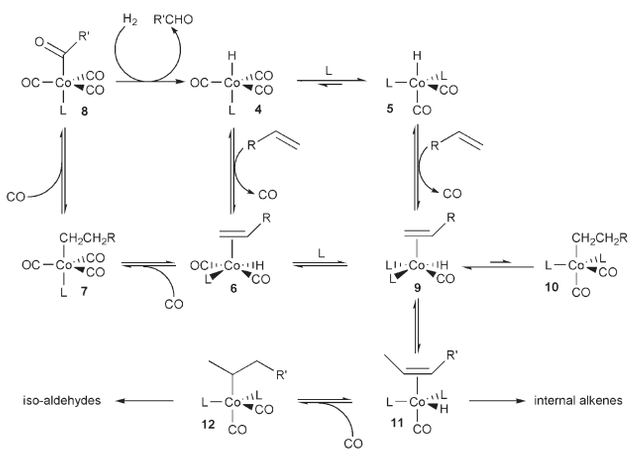

Scheme 3 Proposed mechanism for $P(OPh)_3$ modified cobalt hydroformylation.

The disubstituted hydride **5** is the dominant species under these conditions, and coordination of 1-pentene, followed by hydride insertion, will form the alkyl species $[(C_5H_{11})Co(CO)_2\{P(OPh)_3\}_2]$. Alkyl migration, to yield the acyl species, is probably less favoured than shifting the equilibrium back to the π-complex **9**, as depicted in Scheme 3. This can result in a shift of the terminal double bond towards the internal positions, mainly the C2 position. The internal alkenes thus formed are expected to be less reactive than 1-pentene, leading to poor conversion and low TOF.

Since $[HCo(CO)_4]$ (**3**) is believed to isomerise internal alkenes in a "chain-running" mechanism,[35] one would expect reasonable conversions if unmodified hydride **3** was present. However, with a $[P(OPh)_3]/[Co]$ ratio higher than 4, the formation of the unmodified hydride **3** was suppressed according to HP-IR (not HP-NMR). The decrease in aldehyde formation with increasing ligand excess, and the very low TOF, therefore accounts for the absence of **3** under these conditions. A blank experiment without the addition of ligand (entry 20) supports that assumption. The TOF of the unmodified catalyst was six times higher than for the modified one, whereas the selectivity towards the linear aldehyde was doubled by addition of ligand. At $[P(OPh)_3]/[Co]$ ratios higher than 2, the selectivity varied in a narrow range between 3.6 and 4.6.

As expected, the cobalt phosphite system did not hydrogenate the aldehydes and alkenes, as indicated by the small amount of hexanols formed (< 1%) and pentane (< 0.2%) when using $[P(OPh)_3]/[Co] > 4$. The overall linearity of the aldehydes formed is reasonably good compared to other modified cobalt systems.[5,8,9]

Using 1-heptanol instead of paraffin as solvent (entry 26, Table 6), no significant gas uptake was observed at 140 °C. GC analysis of the reaction mixtures showed no hydroformylation products. No conversion was observed, even under typical conditions (170 °C, 80 bar) for cobalt catalysed hydroformylation (entry 27, Table 6). This corresponds to the HP-IR experiments where no conversion was observed when the species having a strong absorbance at ν_{CO} 1969 cm^{-1} was present (entry 15 and 16, Table 5) in 1-heptanol.

Conclusions

The cobalt complex $[Co_2(CO)_6\{P(OPh)_3\}_2]$ (**2**) has been synthesised in good yield and characterised by IR and NMR, and was structurally characterised. Proposed hydride intermediates $[HCo(CO)_3P(OPh)_3]$ (**4**) and $[HCo(CO)_2\{P(OPh)_3\}_2]$ (**5**) have been synthesised and characterised by IR and NMR. The crystal structure for compound **5** has also been reported. Due to the low thermal stability, no elemental analysis or mass spectrometric data could be obtained for **4** and **5**.

The dimer **2** was used as precursor in the hydroformylation of 1-pentene. HP-IR and HP-NMR studies revealed that under reaction conditions (140 °C and 50 bar) the dominant species is not the monosubstituted hydride **4** but the unsubstituted **3** and the disubstituted hydride **5**. The HP-IR studies revealed that at $[P(OPh)_3]/[Co]$ ratios higher than 4, only the hydrides **4** and **5** are present while the unmodified hydride **3** was observed in the HP-NMR experiments, even at $[P(OPh)_3]/[Co] = 8$. The results from batch autoclave experiments account for the presence of mono- (**4**) and disubstituted (**5**) hydrides, since the activity of $[HCo(CO)_4]$ (**3**) is higher than the activity for $[HCo(CO)_3P(OPh)_3]$ (**4**). Very low TOF was obtained as

well as fair selectivities. The large amount of internal alkenes was explained by the isomerisation nature of the disubstituted hydride $[HCo(CO)_2\{P(OPh)_3\}_2]$ (**5**).

The investigated monodentate phosphite $P(OPh)_3$ was too small in terms of steric demand (cone angle) to form a stable monosubstituted hydride under the reaction conditions. The narrow range with regard to temperature and ligand excess makes triphenylphosphite unsuitable as ligand for cobalt catalysed hydroformylation. Current research is focussing on modification of steric and electronic properties of various phosphites in order to shift the equilibria at reaction conditions towards the desired $[HCo(CO)_3P(OR)_3]$.

Acknowledgements

Financial assistance from SASOL (including post-doctoral funding for MH and RM) and the Research Funds of RAU and the University of Cape Town is gratefully acknowledged. Part of this material is based on work supported by the South African National Research Foundation under Grant number (GUN 2053397). Any opinion, findings and conclusions or recommendations expressed in this material are those of the authors and do not necessarily reflect the views of the NRF.

The Universities of the Witwatersrand (Prof. D. Levendis, Dr. D. Billing) and Cape Town (Prof. L. R. Nassimbeni) are thanked for the use of their diffractometers. Dr. Hong Su (UCT) and Mr. Alfred J. (Fanie) Muller (RAU) are thanked for the data collections and structure analyses. Mr. K. Mokheseng (SASOL: GC analyses) and Mr. J. A. Vorster (RAU; assistance with HP-NMR experiments) are also acknowledged. Drs. Mike Green, C. Grove and C. Crause are thanked for helpful discussions.

References

1 O. Roelen, *Ger. Pat.*, 949 548, 1938.
2 C. D. Frohning and C. W. Kohlpaintner, in *Applied Homogeneous Catalysis with Organometallic Compounds*, eds. B. Cornils and W. A. Herrmann, VCH, Weinheim, 1996, vol. 1, p.29.
3 L. H. Slaugh and R. D. Mullineaux, *US Pat.,* 3.239.569, 1966.
4 L. H. Slaugh and R. D. Mullineaux, *US Pat.,* 3.239.570, 1966.
5 L. H. Slaugh and R. D. Mullineaux, *J. Organomet. Chem.*, 1968, **13**, 469.
6 M. Beller, B. Cornils, C. D. Frohning and C. W. Kohlpainter, *J. Mol. Catal. A: Chem.*, 1995, **104**, 17.
7 (*a*) R. F. Heck and D. S. Breslow, *Chem. Ind. (London)*, 1960, 467; (*b*) R. F. Heck and D. S. Breslow, *J. Am. Chem. Soc.*, 1961, **83**, 4023.
8 J. P. Steynberg, K. Govender and P. J. Steynberg, *World Pat.*, 2002014248, 2002.
9 C. Crause, L. Bennie, L. Damoense, C. L. Dwyer, C. Grove, N. Grimmer, W. Janse van Rensburg, M. M. Kirk, K. M. Mokheseng, S. Otto and P. J. Steynberg, *Dalton Trans.*, 2003, 2036.
10 J. K. Merzweiler and H. M. Tenney, *US Pat.,* 3351666, 1967.
11 D. F. Shriver, M. A. Drezdzon, *The Manipulation of Air-sensitive Compounds*; Wiley-Interscience, New York, 1986.
12 D. D. Perrin, W. L. F. Armarego, *Purifiction of Laboratory Chemicals*, Pergamon Press, Oxford, 1988.
13 The structure of **2** has previously been reported in a thesis: J. A. M. Case, *Dissertation Abstr. B*, 1968, **28**, p. 2786.
14 *COLLECT, Data Collection Software*, Nonius B.V., Delft, The Netherlands, 2000.
15 Z. Otwinoski and W. Minor, *Methods in Enzymology*, 1997, **276**, 307.
16 *SAINT*, Siemens Analytical X-ray Instruments Inc., Madison, Wisconsin, USA, 1995.
17 *Siemens, SADABS*, Siemens Analytical X-ray Instruments Inc., Madison, Wisconsin, USA.
18 G. M. Sheldrick, *SHELXL97, Program for solving Crystal structures*, University of Göttingen, Göttingen, Germany, 1997.
19 K. Brandenburg and M. Berndt, *DIAMOND*, 1999, Version 2.1c. Crystal Impact GbR, Bonn, Germany.
20 C. Loubscher and S. Lotz, *Inorg. Synth.*, 1992, **29**, 178.
21 (*a*) W. Hieber and E. Lindner, *Chem. Ber.*, 1961, **94**, 1417; (*b*) E. J. Moore, J. M. Sullivan and J. R. Norton, *J. Am. Chem. Soc.*, 1986, **108**, 2257.
22 W. Hieber and H. Duchatsch, *Chem. Ber.*, 1965, **98**, 2530.
23 W. Rigby, R. Whyman and K. Wilding, *J. Phys. E.*, 1970, **3**, 572.
24 (*a*) D. C. Roe, *J. Magn. Res.*, 1985, **63**, 388; (*b*) I. T. Horváth and J. M. Miller, *Chem. Rev.*, 1991, **91**, 1339.
25 (*a*) G. G. Summer, H. P. Klug and L. E. Alexander, *Acta Cryst.*, 1964, **17**, 732; (*b*) P. C. Leung and C. Coppens, *Acta Cryst.*, 1983, **B39**, 535.
26 D. H. Farrar, A. J. Lough, A. J. Poë and T. A. Stromnova, *Acta Cryst.*, 1995, **C51**, 2008.
27 (*a*) J. A. Ibers, *J. Organomet. Chem.*, 1968, **14**, 423; (*b*) R. F. Bryan and A. R. Manning, *Chem. Commun.*, 1968, 1316.
28 R. A. Jones, M. H. Seeberger, A. L. Stuart, B. R. Whittlesey and T. C. Wright, *Acta Crystallogr.*, 1986, **C42**, 399.
29 D. Zhao and L. Brammer, *Inorg. Chem.*, 1994, **33**, 5897.
30 T. Bartik, T. Krummeling, B. Happ, A. Sieker, L. Marko, R. Boese, R. Ugo, C. Zucchi and G. Palyi, *Catal. Lett.*, 1993, **19**, 383.
31 J. S. Leigh and K. H. Whitmire, *Acta Crystallogr.*, 1989, **C45**, 210.
32 C. A. Tolman, *Chem. Rev.*, 1977, **77**, 313.
33 C. D. Frohning and C. W. Kohlpaintner, in *Applied Homogeneous Catalysis with Organometallic Compounds*, eds. B. Cornils and W. A. Herrmann, VCH, Weinheim, 1996, vol. 1, p. 75.
34 R. Meijboom, M. Haumann and A. Roodt, unpublished results.
35 Unmodified cobalt catalysed hydroformylation of internal alkenes gives terminal aldehydes and approximately the same l/b ratio as the hydroformylation of terminal alkenes, suggesting that fast isomerisation (to the terminal position) after hydrometallation takes place. This is a well known mechanism in other transition metal complexes and has been extensively studied for, for example, zirconium complexes. This isomerisation chemistry has, however, not been well studied for Co complexes.